Article

Preparation and Infrared/Raman Classification of 630 Spectroscopically Encoded Styrene Copolymers

Hicham Fenniri, Sangki Chun, Owen Terreau, and Juan-Pablo Bravo-Vasquez

J. Comb. Chem., **2008**, 10 (1), 31-36• DOI: 10.1021/cc7001292 • Publication Date (Web): 21 November 2007

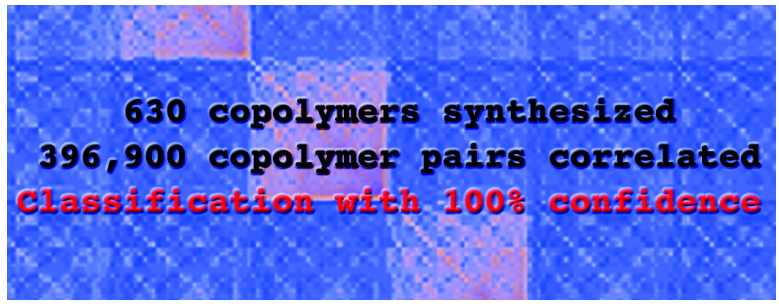

Articles

Preparation and Infrared/Raman Classification of 630 Spectroscopically Encoded Styrene Copolymers

Hicham Fenniri,* Sangki Chun,† Owen Terreau, and Juan-Pablo Bravo-Vasquez

National Institute of Nanotechnology, National Research Council (NINT-NRC), and Department of Chemistry, University of Alberta, 11421 Saskatchewan Drive, Edmonton, Alberta T6G 2M9, Canada

Received August 6, 2007

The barcoded resins (BCRs) were introduced recently as a platform for encoded combinatorial chemistry. One of the main challenges yet to be overcome is the demonstration that a large number of BCRs could be generated and classified with high confidence. Here, we describe the synthesis and classification of 630 polystyrene-based copolymers prepared from the combinatorial association of 15 spectroscopically active styrene monomers. Each of the 630 copolymers displayed a unique vibrational fingerprint (infrared and Raman), which was converted into a spectral vector. To each of the 630 copolymers, a vector of the known (reference) composition was assigned. Unknown (prediction) vectors were decoded using multivariate data analysis. From the inner product of the reference and prediction vectors, a correlation map comparing 396 900 copolymer pairs (630 × 630) was generated. In 100% of the cases, the highest correlation was obtained for polymer pairs in which the reference and prediction vectors correspond to copolymers prepared from identical styrene monomers, thus demonstrating the high reliability of this encoding strategy. We have also established that the spectroscopic barcodes generated from the Raman and infrared spectra are independent of the copolymers' morphology (beaded versus bulk polymers). Besides the demonstration of the generality of the polymer barcoding strategy, the analytical methods developed here could in principle be extended to the investigation of the composition and purity of any other synthetic polymer and biopolymer library, or even scaffold-based combinatorial libraries.

Introduction

Bead-based arrays are rapidly gaining prominence as an assay platform for biorecognition, as they address some of the limitations posed by conventional assay methods. For instance, advantages offered by bead-based arrays include: (a) amenability to high-throughput screening and multiplexing; (b) larger surface areas for receptor conjugation relative to 2D substrates; (c) better accessibility of the analytes to the entire sample volume for interaction with the bead-conjugated receptors; and (d) greater versatility in sample analysis and data acquisition. With these elements in mind, the barcoded resins (BCRs) were introduced as a platform for resin-supported encoded combinatorial chemistry and clinical diagnostics.[1–3] Each BCR features a unique vibrational spectrum (spectroscopic barcode) that can be used to identify the BCR and its cargo using infrared or Raman hyperspectral imaging/mapping,[2] and/or TOF-SIMS imaging.[3] In conjunction with a directed sorting strategy[4] at the single bead level, automated library synthesis in which each compound is assigned a unique barcode is now achievable. Furthermore, this approach offers the opportunity to vary the loading, size, and number of beads representing a given compound barcode. As a result, the quantity of each synthetic intermediate and library member could be tuned to carry out routine spectroscopic characterizations at any stage of the library synthesis and on-bead or solution phase biological evaluations. However, such a strategy engenders two major challenges: (a) a device for rapid barcode reading and bead sorting is necessary[5] and (b) the repertoire of usable BCRs must be expanded. This paper addresses the latter problem.

We have previously reported on the preparation of 25 BCRs from 6 spectroscopically active styrene monomers. These polymers were thoroughly characterized by Raman, infrared, $^{1}H/^{13}C$ NMR spectroscopies and differential scanning calorimetry. Swelling properties, solid-phase peptide synthesis, and on-bead streptavidin-alkaline phosphatase (SAP) binding assay further established that the physical and chemical properties of these BCRs where not altered by the diversity of their encoded polystyrene core. Each of the 25 resins displayed a unique Raman and infrared vibrational fingerprint, which was converted into a "spectroscopic barcode" where the position of each bar matches the peak

* Corresponding author. Tel.: (780) 641-1750. Fax: (780) 641-1601. E-mail hicham.fenniri@ualberta.ca.

† Current address: LG Chem Research Park, 104-1 Moonji-dong, Yuseong-gu, Daejeon 305-380, Korea.

10.1021/cc7001292 CCC: $40.75
Published on Web 11/21/2007

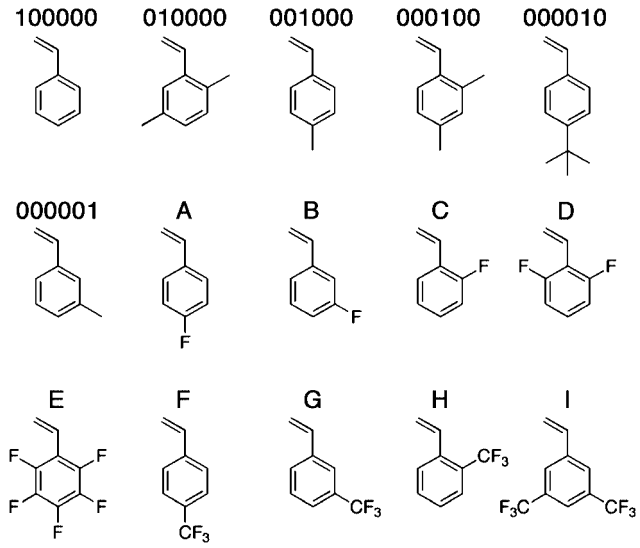

Figure 1. Styrene monomers used to generate a library of 630 spectroscopically encoded polymers.

wavenumber in the corresponding spectrum, independent of the peak intensity. From this simplified representation, similarity maps comparing 35 000 resin pairs were generated to establish the spectroscopic barcoding as a reliable encoding methodology. In effect, in 99% of the cases, the highest similarity coefficients were obtained for resin pairs prepared from the same styrene derivatives.

Here, we report on the synthesis of 630 copolymers prepared from the combinatorial association of 15 spectroscopically active styrene monomers (Figure 1) and their classification with 100% confidence using multivariate data analysis. To expedite the synthesis and demonstrate our ability to generate large libraries of encoded BCRs, we have also shown that the spectra are independent of the polymer morphology (beaded versus bulk polymers).

Materials and Methods

Materials. The styrene monomers and benzoyl peroxide (BPO) were purchased from Aldrich. The monomers were distilled under reduced pressure to remove the radical stabilizer and were stored at 4 °C. CCl_4 (Aldrich) was used to dissolve the copolymers because it is Raman inactive and shows simple infrared spectra. Kimble glass vials (2 mL, 12 mm × 35 mm vials) were used as reactors. Test tubes (25 mL) for polymer precipitation were obtained from VWR or Fisher Scientific.

Strategy for the Preparation of Spectroscopically Encoded Polymers. The six alkylated styrene monomers were combined in a binary fashion resulting in 63 ($2^n - 1$) polymers as shown in Table 1. The same sublibrary was resynthesized by including one of the fluorinated monomers (A−I) thus resulting in 9 additional sublibraries and a total of 630 copolymers (10 × 63). We have arbitrarily assigned a basic six-digit binary code for each alkylated styrene monomer (100000, 010000, 001000, 000100, 000010, 000001). The presence (1) or absence (0) of a particular monomer within a given polymer determines the binary code of the barcoded polymer. For instance, polymer 100100 is composed of monomers 100000 and 000100 in equal proportions (50/50). The appearance of a letter at the beginning of the binary code signals the nature of the fluorinated monomers used. For instance, polymer F-100100 contains monomer F (10%) in addition to 100000 and 000100 in equal proportions (45/45). Thus, except for sublibrary L1 that does not have a fluorinated styrene monomer, all polymers have a seven-digit alphanumeric code. Fluorinated styrene monomers A−I were used in the preparation of sublibraries L2−L10, respectively.

Table 1. Styrene Monomer Composition of Polymer Sublibrary L1[a]

P1 (BCR1): 100000	**P2 (BCR10):** 001000	**P3 (BCR25):** 000001
P4: 000100	**P5 (BCR22):** 010000	**P6:** 000010
P7 (BCR13): 101000	**P8 (BCR16):** 100001	**P9 (BCR18):** 100100
P10 (BCR24): 110000	**P11 (BCR8):** 100010	**P12 (BCR11):** 001001
P13: 001100	**P14 (BCR14):** 011000	**P15 (BCR12):** 001010
P16: 000101	**P17 (BCR7):** 010001	**P18 (BCR21):** 000011
P19: 010100	**P20:** 000110	**P21 (BCR19):** 010010
P22 (BCR9): 101001	***P*23:** 101100	**P24 (BCR23):** 111000
P25 (BCR20): 101010	**P26:** 100101	**P27 (BCR2):** 110001
P28 (BCR3): 100011	**P29:** 110100	**P30:** 100110
P31 (BCR5): 110010	**P32:** 001101	**P33 (BCR6):** 011001
P34 (BCR17): 001011	**P35:** 011100	**P36:** 001110
P37 (BCR15): 011010	**P38:** 010101	**P39:** 000111
P40 (BCR4): 010011	**P41:** 010110	**P42:** 010111
P43: 011110	**P44:** 011011	**P45:** 001111
P46: 011101	**P47:** 110110	**P48:** 110011
P49: 100111	**P50:** 110101	**P51:** 111010
P52: 101110	**P53:** 111100	**P54:** 101011
P55: 111001	**P56:** 101101	**P57:** 011111
P58: 110111	**P59:** 111110	**P60:** 111011
P61: 101111	**P62:** 111101	**P63:** 111111

[a] P1−P63 refer to the 63 polymers of sublibrary L1. Sublibraries L2−L10 have exactly the same composition in addition to ca. 10 mol % of fluorinated styrene monomers A−I, respectively. BCR1−BCR25 refer to previously prepared polymers in beaded format.[1a]

Up to six alkylated styrene monomers in equimolar amount, one fluorinated monomer (10 mol %), and 0.5 mg BPO were combined in a 2 mL glass vial. The vials were vortexed for 1 min and then placed in a preheated (70 °C) aluminum block. After 2 h, the heating was stopped and CCl_4 (1 mL) was added to each reactor to dissolve the bulk polymer. The polymer solution was transferred into a 25 mL test tube containing CH_3OH (5 mL) and vortexed to ensure complete precipitation of the polymer. The suspension was sonicated for 1 h, filtered, and dried under vacuum. Table 1 shows the composition of the polymers prepared in powder and beaded format.

Fourier Transform Infrared (FTIR) Spectroscopy. The bulk copolymers and dry KBr were thoroughly ground in a smooth agate mortar and pressed to form a pellet. The infrared spectra (4000–400 cm^{-1}) were recorded under nitrogen on a Nicolet Nexus 870 spectrometer with a resolution of 4 cm^{-1}. All the spectra were baseline corrected and normalized with built-in Nicolet Omnic 5.1 software. FTIR spectra of the beaded copolymers were recorded on a Varian Stingray imaging spectrometer with 8 cm^{-1} spectral resolution. This instrument consists of a UMA 600 microscope coupled to an FTS 7000 rapid scan interferometer, equipped with a motorized (x,y,z) sample holder. The acquisition time was ∼20 s (16 scans/bead).

Raman Spectroscopy. The Raman spectra (1600–450 cm^{-1}) were recorded on a Thermo Nicolet dispersive Raman

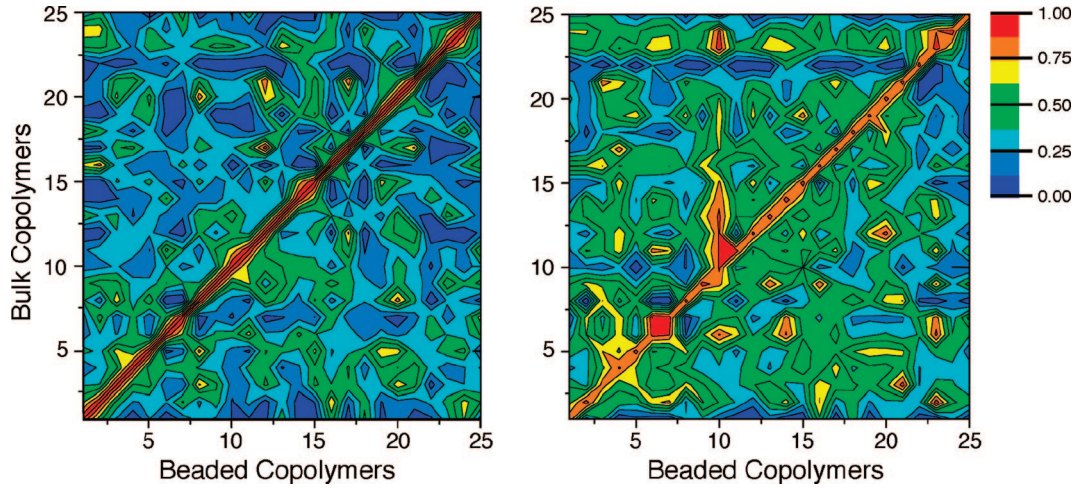

Figure 2. Infrared (A) and Raman (B) similarity contour plots showing high spectral similarity between bulk and beaded copolymers.

spectrometer with an exposure time of 1 s (4 scans per spectrum) and a spectral resolution of 4 cm^{-1}. All the spectra were baseline corrected and normalized with built-in Nicolet Omnic for Almega (v7.1). The samples were placed in the microscope compartment under a 10× objective on a glass slide immobilized on the microscope stage with a piece of double-sided tape. A frequency doubled Nd:YY04 DPSS green laser (532 nm) with a beam diameter of 1.9 mm was used as an excitation source for the sample. The scattered light was detected on a charge-coupled device (CCD) detector.

Results and Discussion

The vibrational fingerprint is independent of the polymer format. To expedite library synthesis, we opted for bulk polymerization rather than suspension polymerization, as the latter requires optimization[1a,b] and larger amounts of starting materials. However to validate this strategy, we had to establish that a significant subset of polymers prepared by the two methods still have similar spectra. Thus, 25 copolymers of identical composition to a previously reported bead library[1a] were included in sublibrary L1. Two methods were used to compare the two sets of spectra. The first consists in converting the Raman and infrared spectra of the beaded and bulk copolymers into spectroscopic barcodes[1a,b] and calculating a similarity coefficient (S)[1a,6] between each copolymer pair according to eq 1

$$s = \frac{\sum_i (V_{i\mathrm{A}} V_{i\mathrm{B}})}{\sum_i V_i + \sum_i V_i - \sum_i (V_{i\mathrm{A}} V_{i\mathrm{B}})} \qquad (1)$$

where $V_{i\mathrm{A}}$ is 1 when vibration i is present in polymer A and 0 when it is absent. Similarly, $V_{i\mathrm{B}}$ is 1 when vibration i is present in copolymer B and 0 when it is not. Thus, the numerator corresponds to the intersection of the family of vibrations present in A with the family of vibrations present in B (i.e., number of vibrations common to both copolymer A and copolymer B). The denominator corresponds to the union of families A and B (i.e., sum of the vibrations unique to copolymer A, the vibrations unique to copolymer B, and the vibrations common to both copolymers). To simplify the comparison of the resulting Raman and infrared similarity tables, the S values were normalized along each column relative to the diagonal values. The resulting normalized tables were then presented as contour plots in which the highest similarity intersections appear in red and the lowest appear in blue (Figure 2).

Several important conclusions were drawn from this analysis. First, both the infrared and Raman contour plots show the highest similarity along the diagonal, demonstrating that beaded and bulk copolymers with identical binary codes maintain the highest level of similarity. The high average similarity along the diagonal (0.88 for infrared, 0.98 for Raman) relative to the average off-diagonal values (0.31 for infrared, 0.44 for Raman) further demonstrates the uniqueness of the vibrational spectra. This uniqueness, in turn, suggests that any number "n" of carefully selected styrene monomers could in principle result in $2^n - 1$ unique copolymers. Second, the infrared and Raman contours are significantly different therefore allowing us to use them synergistically for the unequivocal identification of a barcoded copolymer.

The second method applied to the Raman data (but could also be extended to the infrared data) uses correlation maps.[2b] The 25 beads were placed in 5 rows of 5 beads on a piece of double-sided tape (Figure 3A) and were mapped as previously described.[2b] The Raman instrument software (Omnic) is equipped with a program that correlates each spectrum in the map to a spectrum in a pre-existing library of the 630 bulk copolymers' spectra. In this case, the correlation of the Raman map to the spectra of sublibrary L1 confirmed the highest correlation between beads and bulk copolymers with the same monomer composition. For instance, Figure 3B shows the correlation map between all 25 beads and bulk polymer 100100 and points particularly to the fact that the highest correlation is with BCR#18 (white arrow), in agreement with the correlation given in Table 1. Similar mapping results were obtained for all 25 BCRs and corresponding bulk copolymers (data not shown).

Multivariate Data Analysis. After establishing that the vibrational fingerprint is independent of the polymer's format, we set out to demonstrate that any of the 630 copolymers synthesized could be identified with 100% confidence.

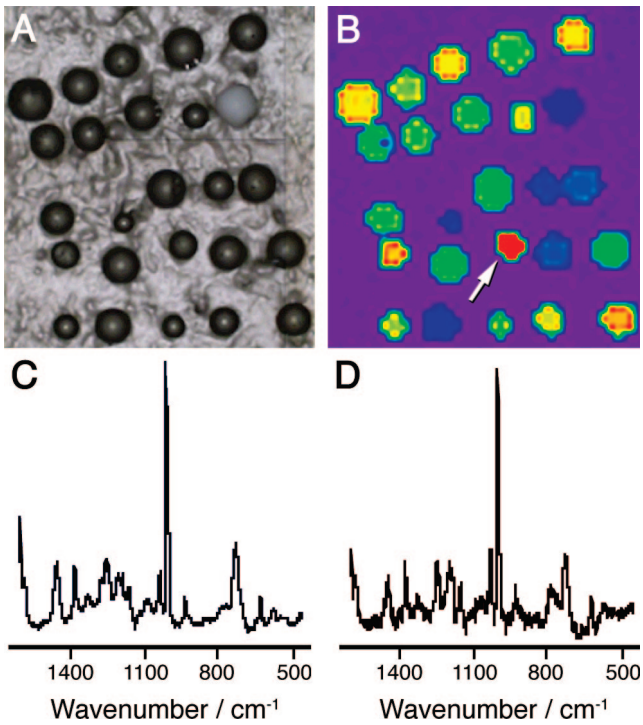

Figure 3. Video image of 25 beads (A) and Raman correlation map (B) of 25 BCRs based on the Raman spectrum of bulk copolymer 100100 (reference). The Raman spectra of copolymer 100100 in the bead (C) and bulk (D) forms are essentially identical.

Multivariate data analysis was used to classify the Raman and infrared spectra as follows: (a) A reference identity matrix, **Y**, was generated. This matrix consists of 630 copolymers (rows) × 15 monomers (columns), in which each coordinate was assigned based on the mass ratio of monomers within the copolymer. (b) A spectral matrix, **X**, comprising 630 copolymers (rows) × 1868 wavenumbers per infrared spectrum (columns), was generated. Each coordinate in this matrix contained the absorbance reading at a given wavenumber for a given copolymer. (c) Using the Unscrambler software package (Camo),[7] a partial least-squares regression (PLS2) model that correlates these two matrices was generated. (d) The regression model was validated by generating a predicted identity matrix (**Y′**) from the spectral matrix (**X**) and correlating it to the reference identity matrix (**Y**). The correlation between **Y** and **Y′** was obtained from the inner product (eq 2) of the 15 dimensional reference composition vectors y_i and the predicted identity vectors y_i' unique to each copolymer. The angular matrix composed of 396 900 (630 × 630) θ angles resulting from the inner product of **Y** and **Y′** was then converted to a contour plot for better visualization.

$$\cos\theta = \frac{y_i \cdot y_i'}{|y_i||y_i'|} \qquad (2)$$

Conservation of the Vibrational Barcodes. From the partial least-squares regression model, 15 unique dimensional vectors were assigned to each infrared spectrum of the 630 copolymers. To estimate the prediction error in the validation stage, a test set composed of 255 spectra out of 630 was randomly chosen and the validation variance was calculated. The variable set in the **X** matrix was optimized from the standard deviation of the difference between the reference and prediction vectors after each data processing by the following: (a) omission of the 2000–2600 and 3200–4000 cm^{-1} range and (b) first and second derivatization of the spectra. The standard deviations with and without the given spectral range were 3.9 and 3.5, respectively. The standard deviations after the first and second derivatization were calculated to be 4.4 and 4.9, respectively. Therefore, for the final model, the normalized infrared spectra were chosen with fixed ranges from 400 to 2000 and 2600 to 3200 cm^{-1}. Because of the low mass ratio of fluorinated styrene monomers (ca. 10%) in the copolymer libraries, its spectral intensity was generally ~3 times smaller than the average intensity of the other monomers in any given copolymer. Thus, to compensate for their relatively small vector contribution, the composition of fluorinated monomers in the **Y** matrix was weighted by a factor of 3.

After this validation stage, the reference (**Y**) and spectral (**X**) matrices were generated and correlated using a PLS2 model. To demonstrate our ability to classify the infrared spectra with high confidence, the spectral matrix (**X**) and the regression model were used to generate matrix **Y′** of predicted composition vectors for the 630 copolymers. The prediction was then validated by calculating the inner product of the reference composition vectors y_i and the predicted identity vectors y_i' unique to each copolymer. Since each copolymer has a unique composition vector with a unique direction in 15-dimensional vector space, the θ value between the reference and prediction vectors approaches 0 only for copolymers with identical composition. For example, the reference and prediction composition vectors for spectral element 100010 are (50,0,0,0,50,0,0,0,0,0,0,0,0,0,0) and (50.4,−6.2,2.1,−3.7,54.5,−5.9,5.4,6.6,11.7,3.8,0.8,2.2,−2.3,−1.6,−0.5), respectively. The θ value from their inner product is 14°, which is the smallest angle between this reference vector and any prediction vector. For better visualization, the angular matrix composed of 396 900 (630 × 630) θ angles resulting from the inner product of **Y** and **Y′** was then converted into a contour plot (Figure 4). Without exception, the lowest θ values (highest correlation) were obtained for copolymer pairs in which the reference and prediction vectors correspond to copolymers with identical monomer composition. The θ values averaged 8° along the main diagonal of the contour plot, whereas off-diagonal values averaged 68°.

Figure 4A revealed several interesting characteristics. First, the correlation plot appears to be divided into 100 smaller squares (10 × 10), each representing the correlation map between sublibrary pairs (10 × 10). The similarities observed between sublibraries are due to the fact that they are identical except for the fluorinated monomer (ca. 10% w/w). For example, the first member of sublibrary L1 has the same composition as the first member of sublibrary L2 except that sublibrary L2 contains an additional fluorinated monomer. This also explains why sublibrary L1 correlates better with all other sublibraries (L2−L10). Second, while the diagonal values within each of the 100 squares correspond to low θ values (local minima), the matrix main diagonal corresponds to globally lower θ values. The appearance of a global

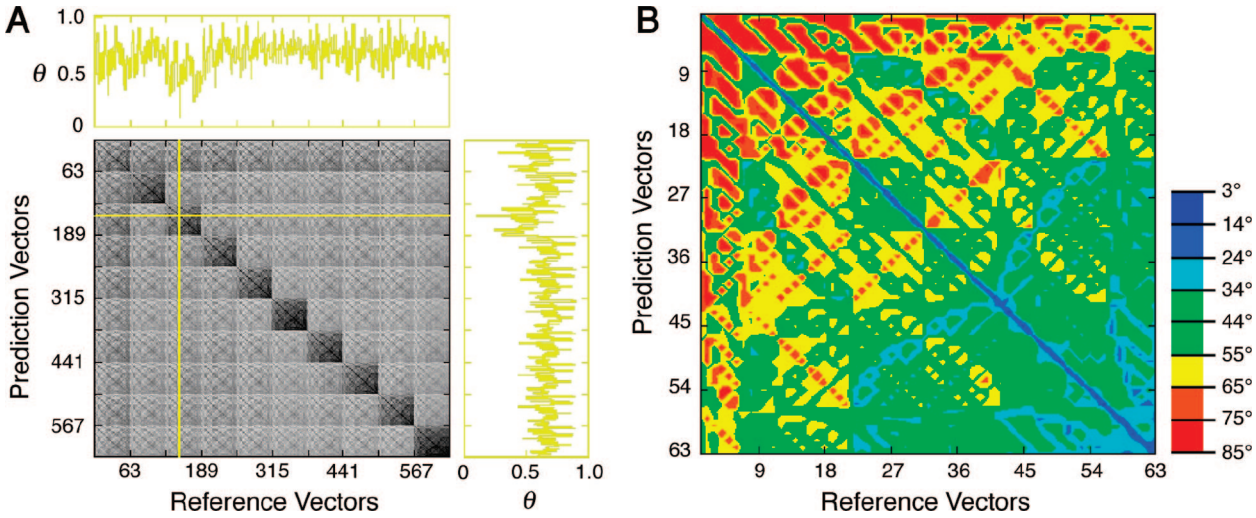

Figure 4. Conservation of the infrared barcode. (A) Infrared correlation map shown as a contour plot correlating 396 900 copolymer pairs (630 × 630). (B) Expansion of the top left square corresponding to sublibrary L1, where the low θ values (blue regions) correspond to the highest correlations and the high θ values (red regions) correspond to the lowest correlations.

minimum along the main diagonal shows that the predicted vectors for the 630 copolymers are most similar to the reference vectors that represent copolymers with identical monomer composition. Within a given sublibrary, an increment in the number of monomers decreases θ values. For instance, the reference vector for copolymer 100000 and the prediction vector for copolymer 010000 are orthogonal ($\theta = 90°$, no correlation), whereas the θ value between 111011 and 101111 is 40° because they share four vector components. However, this value is still higher than the diagonal θ values for 111011 (11.3°) and 101111 (12.1°) confirming that copolymers with identical composition always result in the lowest θ values (highest correlation).

In addition to infrared classification of the copolymers, we have also carried out the same analysis with Raman scattering. There are several advantages to using Raman spectroscopy to identify the BCRs. First, Raman scattering spectra are not influenced by water and physiological media, which are necessary for biomolecular recognition. Second, Raman scattering provides not only the vibrational modes of the molecule under study but also its electronic emission spectrum (fluorescence). Although this effect is usually an obstacle in the normal practice of Raman scattering spectroscopy,[8] we have recently demonstrated that fluorescence emission and Raman scattering could be recorded on the same instrument using two laser lines.[1c] This process should expedite biomolecular screening and the BCR classification process.

The Raman spectra were processed in exactly the same manner as the infrared spectra (vide supra), and a correlation map was generated (Figure 5). The θ values along the main diagonal averaged 11°, whereas off-diagonal values averaged 60°, which confirms the reliability of the Raman classification method. In effect, cross-correlation of all the polymers (396 900 pairs) showed that, with the exception of 20 copolymers out of 630, the lowest θ values (highest correlations) were obtained for the copolymer pairs in which the reference and prediction vectors correspond to copolymers with identical monomer composition. For the 20 inaccurate diagonal classifications, the θ values were second

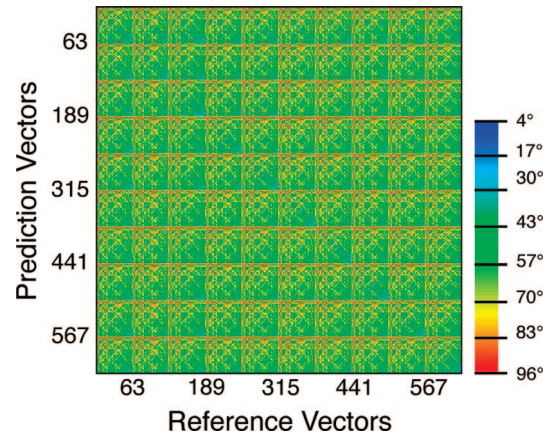

Figure 5. Conservation of the Raman barcode. The Raman correlation map is shown as a contour plot correlating 396 900 copolymer pairs (630 × 630), where the low θ values (blue regions) correspond to the highest correlations and the high θ values (red regions) correspond to the lowest correlations.

lowest because the fluorinated monomer was incorrectly classified in the vector spectra. The lowest θ values in these 20 cases were incorrectly obtained for copolymer pairs belonging to sublibrary L1, which lacks the fluorinated monomer. This analysis shows also that elimination of this subset from the polymer library would ensure classification with 100% confidence. This is a remarkable result given that Raman spectroscopy is far less sensitive than infrared spectroscopy and given that the fluorinated monomers incorporated in ca. 10% w/w in the copolymers are structurally similar to the other monomers used.

Finally, all observations made for the infrared correlation plot (Figure 4) apply also for the Raman correlation plot (Figure 5). Notably, (a) the correlation plot appears to be divided into 100 smaller squares (10 × 10), each representing the correlation map between sublibrary pairs (10 × 10) and (b) the diagonal values within each of the 100 squares correspond to local minima, whereas the matrix's main

diagonal corresponds to globally lower θ values in 99.995% of the cases.

Conclusion

The BCR concept introduces a new paradigm in combinatorial chemistry, as the beads are no longer just carriers for solid-phase synthesis but are in addition the repository of the synthetic scheme to which they were subjected. In conjunction with a directed sorting strategy *at the single bead level*,[4] automated target-oriented synthesis and diversity-oriented synthesis of libraries in which each compound is assigned a unique barcode at the outset of a split-pool synthesis are now achievable. Such a strategy engenders several challenges, many of which have been solved thus far. For instance, we have established the reliability of the spectroscopic barcoding approach[1] and have shown that the diversity of the polymer core does not adversely affect on-bead binding assays and reactivity on the BCRs.[1a] We have also shown that hyperspectral imaging/mapping[2] and TOF-SIMS imaging[3] could be used to expedite BCR identification and classification on a 2D substrate. Before proceeding to any significant application of this platform in for instance drug discovery, biomedical diagnostics, or cross-reactive sensor arrays, we had to demonstrate that (a) the repertoire of usable BCRs can be expanded and (b) the BCRs could be sorted rapidly. In this report, we have established that a large number of spectroscopically encoded polymers could be designed from a small set of styrene monomers. With this capability in hand, and once our efforts to develop a barcode-reading and bead-sorting device are completed, we will be in position to synthesize focused libraries (<1000 members) on the BCRs. In the meantime, our current challenges are to develop surface-enhanced Raman scattering (SERS) active BCRs for ultrafast barcode reading and bead sorting and new families of BCRs with improved swelling properties in a broad range of solvents.

The combination of infrared/Raman spectroscopies and multivariate data analysis allowed us not only to unequivocally identify and classify all the polymers investigated but also to eliminate the polymers that cannot be identified with full confidence. We have also shown that bulk and beaded polymers have essentially the same vibrational signature, thus allowing for facile selection of inexpensive copolymer compositions for BCR synthesis. Finally, the analytical methodology developed here could in principle be extended to the classification of any (bio)polymer or even scaffold-based combinatorial libraries.

Acknowledgment. We thank NRC's Genomics and Health Initiative, the National Institute for Nanotechnology, the University of Alberta, and the National Institutes of Health (NIH EB03824) for supporting this program.

Supporting Information Available. Raman and FTIR spectra of all the polymers synthesized. This material is available free of charge via the Internet at http://pubs.acs.org.

References and Notes

(1) (a) Fenniri, H.; Chun, S.; Ding, L.; Zyrianov, Y.; Hallenga, K. *J. Am. Chem. Soc.* **2003**, *125*, 10546–10560. (b) Fenniri, H.; Ding, L.; Ribbe, A. E.; Zyrianov, Y. *J. Am. Chem. Soc.* **2001**, *123*, 8151–8152. (c) Raez, J.; Blais, D. R.; Zhang, Y.; Alvarez-Puebla, R. A.; Bravo-Vasquez, J. P.; Pezacki, J. P.; Fenniri, H. *Langmuir* **2007**, *23*, 6482–6485.

(2) (a) Fenniri, H.; Hedderich, H. G.; Haber, K. S.; Achkar, J.; Taylor, B.; Ben-Amotz, D. *Angew. Chem., Int. Ed.* **2000**, *39*, 4483–4485. (b) Fenniri, H.; Terreau, O.; Chun, S.; Oh, S. J.; Finney, W.-F.; Morris, M. D. *J. Comb. Chem.* **2006**, *8*, 192–198.

(3) Chun, S.; Xu, J.; Cheng, J.; Ding, L.; Winograd, N.; Fenniri, H. *J. Comb. Chem.* **2006**, *8*, 18–25.

(4) (a) Nicolaou, K. C.; Xiao, X.-Y.; Parandoosh, Z.; Senyei, A.; Nova, M. P. *Angew. Chem., Int. Ed.* **1995**, *34*, 2289–2291. (b) Moran, E. J.; Sarshar, S.; Cargill, J. F.; Shahbaz, M. J. M.; Lio, A.; Mjalli, A. M.; Armstrong, R. W. *J. Am. Chem. Soc.* **1995**, *117*, 10787–10788. (c) Czarnik, T.; Nova, M. *Chem. Brit.* **1997**, *33*, 39–41.

(5) (a) Gao, X.; Nie, S. *Anal. Chem.* **2004**, *76*, 2406–2410. (b) Drenski, M. F.; Mignard, E.; Alb, A. M.; Reed, W. F. *J. Comb. Chem.* **2004**, *6*, 710–716. (c) Trau, M.; Battersby, B. J. *Adv. Mater.* **2001**, *13*, 975–979. (d) Ormerod, M. G., Ed. *Flow Cytometry: A Practical Approach*; Oxford University Press: New York, 2000. (e) Keren, D. F., McCoy, J. P., Jr., Carey, J. L., Eds. *Flow Cytometry in Clinical Diagnosis*; ASCP Press: Chicago, 2001. (f) Rudbruch, A., Ed. *Flow Cytometry and Cell Sorting*; Springer: New York, 2000.

(6) Woodruff, H. B.; Lowry, S. R.; Ritter, G. L.; Isenhour, T. L. *Anal. Chem.* **1975**, *47*, 2027–2030.

(7) Esbensen, K. H.; *Multivariate Data Analysis−in practice*, 5th ed.; Camo Technologies: Woodbridge, NJ, 2002 pp 137–153.

(8) Long, D. A. John Wiley & Sons Ltd: Chichester, 2002.

CC7001292